PARTICLE TRI-AXIAL ROTOR MODEL CALCULATION OF LOWLYING STATES IN THREE ODD-MASS ISOTOPES OF OSMIUM

By; Gashaw Dejene Bogale

Advisor; Dr. Teklemariam Tessema(PhD)

A THESIS SUBMITTED TO

THE DEPARTMENT OF PHYSICS

PRESENTED IN PARTIAL FULFILMENT OF THE
REQUIREMENTS FOR THE DEGREE OF MASTER OF SCIENCE IN PHYSICS
(NUCLEAR PHYSICS) MASTER OF SCIENCE
JIMMA UNIVERSITY
JIMMA, ETHIOPIA
JUNE 2018

JIMMA UNIVERSITY
DEPARTMENT OF
PHYSICS

This is to certify that the thesis prepared by **Gashaw Dejene Bogale** Graduate Studies entitled "**PARTICLE TRI-AXIAL ROTOR MODEL CALCULATION OF LOWLYING STATES IN THREE ODD-MASS ISOTOPES OF OSMIUM**" in fulfillment of the requirements for the degree of **Master of Science** complies with the regulations of the University and meets the accepted standards with respect to originality and quality. .

Dated: June 2018

Supervisor: _____
Dr.Teklemariam

External Examiner: _____

Internal Examiner: _____

JIMMA UNIVERSITY

Date: **June 2018**

Author: **Gashaw Dejene Bogale**

Title: **PARTICLE TRI-AXIAL ROTOR MODEL CALCULATION OF LOWLYING STATES IN THREE ODD-MASS ISOTOPES OF OSMIUM**

Department: **Physics**

Degree: **M.Sc.** Convocation: **January** Year: **2018**

Permission is herewith granted to Jimma University to circulate and to have copied for non-commercial purposes, at its discretion, the above title upon the request of individuals or institutions.

Signature of Author

Table of Contents

}

Abstract

Level energies, gamma transition energies and intensity branching ratios for low-lying states of negative parity low-lying rotational bands of three odd mass Osmium isotopes ,$^{175,177,181}Os$, were calculated within particle triaxial rotor model by using fortran77 based computational codes called GAMPYN, ASYRMO AND PROBAMO. The calculated results of those Osmium isotopes are discussed and compared with experimental data by using tables and figures. It is observed that the PTRM calculation results are in a good agreement with that of experimental data.

Acknowledgement

I would like to thank God for every thing in my way. First and foremost, my advisor, Dr. Teklemariam Tessema(PhD) thank you a lot for providing me a positive and intellectually stimulating research environment that has enabled me to go through a challenging process. I am grateful for your fruitful support, discussions and profound comments.

Also I thank all JU Physics department stuffs and my classmates.

Chapter 1

Introduction

1.1 Background

Many nuclei with N and Z values between magic numbers are permanently deformed in their ground states[1]. The deformation arises because of the way valence nucleons arrange themselves in unfilled shell[3]. Deformed stable nuclei are found throughout the periodic table and are most common in the mass region $150 < A < 190$ and $A > 230$. In the first group protons and neutrons are filling the shells above Z=50 and N=82 and, in the heavier group, shells above $Z = 82$ and $N = 126$ are being filled. The tendency to drive the nucleus into a non-spherical shape is greatest when the shell is about half filled. Beyond this point, additional nucleons are constrained to enter the remaining unfilled sub-states in the shell. Gradually, the tendency to deformation is reversed and sphericity is restored when shell closure is complete[5]. Rotational motion can be observed only in nuclei with non spherical equilibrium shapes[3]. Increasing the total angular momentum corresponds to adding rotational energy to the nucleus and the nuclear excited states form a sequence known as a rotational band. The general structure of the odd-A deformed nuclei is thus characterized by rotational bands built on single particle states calculated from the deformed shell

model potential. In recent years nuclei with deformed shape near closed shells in the high mass region(rare earth and actinides region) has become a subject of great interest. As a result, much of work has been focused on the description of nuclear structure properties of those nuclei by using different nuclear structure models. Among those models, one is particle tri-axial rotor model of [7,8]. This simple model consisting of a particle coupled to a rotor provides an approximate description of many of the properties of the lowlying bands in odd-A nuclei[4]. Since Osmium(Z=76) is found naturally in a highly deformation region mentioned above, I'm interested to calculate its low-lying states of the low-lying rotational bands by using particle tri-axial rotor model.

1.2 Statement of the Problem

Having a detail information about properties of a nuclei is necessary to use the nuclei in an appropriate way and manner. Most of the physical quantities that describe the nuclear structure like level energy, electromagnetic transitions , gamma transition probabilities and so on, have values experimentally measured rather than calculated values. And also from different nuclear data centers or from published journals, the experimental values are more available. As an example, for odd-A osmium isotopes ($^{175,177,181}Os$), the experimental values of level energy and gamma transition probability of the lowlying states of the bands are available on different nuclear data centers but we unable to find theoretical calculation of structure of Osmium isotopes. Therefore, the work was aimed to calculate the level energy, gamma transition energy and gamma branching ratios of the low-lying states of odd-A osmium isotopes ($^{175,177,181}Os$). In doing so, the following questions were answered during this work.

- What are the calculated values of level energy and gamma transition probabilities of lowlying states of odd-mass isotopes of Osmium ($^{175,177,181}Os$))?
- What agreement is there between the calculated values and the experimentally measured value?

1.3 Objectives

1.3.1 General objective

The main objective of this study is to calculate the level energy, gamma transition energy and branching ratios of the lowlying states of three odd mass Osmium isotopes by using particle tri-axial rotor model.

1.3.2 Specific objective

- To calculate the level energy and gamma transition energy of lowlying states of odd-mass osmium isotopes ($^{175,177,181}Os$)
- To calculate the gamma intensity branching ratios.
- To validate the calculation by comparing the calculated values with that of experimental data.

1.4 Significance of the study

Obtaining theoretical data for lowlying states on level energies, gamma transition energies and gamma intensity branching ratio of three odd mass Osmium isotopes by theoretical calculations is the main relevance of this research. In addition this

study can be used as a reference to develop the work further to higher rotational bands of odd mass Osmium isotopes and also could be used as a reference on similar calculations.

1.5 Limitation of the study

- Due to time constraint the study was limited to three odd mass osmium isotopes; $^{175,177,181}Os$.
- Non availability of some experimental data for comparison.
- Less access to internet and lack of related work for reference in the library.

.

Chapter 2

Literature Review

2.1 Nuclear Models

The nucleus, like the atom, has discrete energy levels whose location and properties are governed by the rules of quantum mechanics. The locations of the excited states differ for each nucleus. Each excited state is characterized by quantum numbers that describe its angular momentum, parity, and isospin[9].

Analyzing the interactions among many nucleons to calculate the energy levels and their properties is a complicated task. Instead, nuclear scientists have developed several nuclear models that simplify the description of the nucleus and the mathematical calculations. These simpler models still preserve the main features of nuclear structure[9]. Recently there has been notable success, particularly by Maria Mayer, in explaining many nuclear phenomena including spins, magnetic moments, isomeric states, etc. On the basis of a single particle model for the separate nucleons in a spherical nucleus. The spherical model, however, seems incapable of explaining the observed large quadrupole moments of nuclei. An extension of the logic of this model leads to the prediction that greater stability is obtained for a spheroidal than for a

spherical nucleus of the same volume, when reasonable assumptions are made concerning the variation of the energy terms on distortion[10].

Nuclei have a very regular structure with many general and simple properties that are predicted by quantum mechanical treatment of particles moving in a potential well. Nuclear model is a simplified view of nuclear structure that contains the essentials of nuclear physics[3]. No complete theory exists with fully describes the structure and behavior of complex nuclei based solely on a knowledge of the force acting between nucleons. However, great progress has been and is being made with the aid of conceptual models designed to give insight into the underlying physics of the inherently complex situation. A model embodies certain aspects of our knowledge and, almost invariably, incorporates simplifying assumptions which enable calculations to be made. A successful model should be able to give a reasonable account of the properties it was designed to address and also make predictions of other properties which can be checked by experiment.

2.1.1 Nuclear shell model and independent particle motion

The basis of this model is that there is an ordered structure within the nucleus in which the neutrons and protons are arranged in stable quantum states in a potential well that is common to all of them. Indeed, many nuclei behave as if most of the nucleons form an inert core and low-energy excited states are determined by a few nucleons 'outside' the core. The picture is similar to that of an atom in which electrons are arranged in shells and any chemical activity is determined by the most weakly bound, valence electrons[5]. By independent particle model we refer to the description of a nucleus interms of non interacting particles in the orbits of a spherically symmetric potential U(r), which is itself produced by all the nucleons[1]. Beside a sharp drop in neutron

separation energy and proton separation energy just after magic numbers, the lowest excited states in nuclei with magic numbers(2,8,20,28,50 82,126) of either protons or neutrons are, on average, extremely highlying. In considering an appropriate potential for the nuclear case, a tremendous simplification results if the potential is central, that is if it depends only on the radial distance from the origin to the given point. Then, the angular dependence of a particle wave function is independent of the detailed radial behavior of the central potential[1]. We denote an arbitrary potential by U(r) and only require that U(r) is attractive and U(r)→ 0 as r→0. The schrodinger equation for such a potential is,

$$H\Psi = [\frac{p^2}{2M} + U(r)]\Psi(r) = E_{nlm}\Psi_{nlm}(r) \tag{2.1.1}$$

This equation is separable into radial and regular coordinates and therefore the solutions Ψ_{nlm} can be written

$$\Psi_{nlm}(r) = \Psi_{nlm}(r\theta\phi) = \frac{1}{r}R_{nl}(r)\Psi_{nl}(\theta\phi) \tag{2.1.2}$$

Here, n- is the radial quantum number, l- the orbital angular momentum and m- the eigen value of its z-component, I_z. It is conventional in nuclear physics to give names to different l values following the convention;

$l = 0, 1, 2, 3, 4, 5, ... \ s, p, d, f, g, h, ...$

For a given l, m takes the values $l, l-1, l-2, ..., 0, -1, -2, ...(l-1), -l$. Since U(r) is spherically symmetric the (2I+1)energies are independent of m and we will usually delete this index. The radial Schrodinger equation is,

$$\frac{\hbar^2}{2M}\frac{d^2R_{ln}(r)}{dr^2} + [E_{nl} - U(r) - \frac{\hbar^2}{2M}\frac{l(l+1)}{r^2}]R_{nl}(r) = 0 \tag{2.1.3}$$

Its solutions have some interesting properties. First, outside the potential, the

wave function decreases exponentially and therefore vanishes as r$\rightarrow \infty$. The quantum number n specifies the number of nodes (zeros) of the wave function with the usual, but not universal, convention that one counts the node at infinity but not that at r = 0, that is, n = l,2,.... We now turn to the harmonic potential. This potential is particularly popular in nuclear physics for two principle reasons; 1) It provides a remarkably good approximate solution to many nuclear problems and 2) it is particularly easy to handle mathematically, thus yielding many results analytically. It is simply given by[6],

$$V(r) = \frac{1}{2}M^2w^2r^2 \tag{2.1.4}$$

The eigen values E_{nl} are;

$$E_{nl} = (2n + \frac{1}{2})\hbar\omega \tag{2.1.5}$$

The energy levels of the harmonic oscillator potential are shown in Fig. 2.1. They display two important properties that are evident from the expression for E_{nl}. First, the energy levels fall into degenerate multiplets defined by the (integer) values of $In + 1$. Secondly, a given multiplet generally contains more than one value of the principle quantum number n and of the orbital angular momentum l. A change of 2 units in l is equivalent to a single unit change in n. Thus, as evident in the figure, the levels 3s, 2d, and 1g are all degenerate. Physically, this is entirely reasonable in view of the arguments above concerning the sequencing of energy levels in an arbitrary central potential as a function of n and l. Specifically, since the energy due to centrifugal effects must increase with l as well as with the number of nodes (n) in the wave function, it is clear that, at least qualitatively, one can compensate an increase in n with a decrease in l. The factor connecting these effects is exactly 2 for harmonic oscillator potential: it is also 2 for a square well potential. It is this grouping of

levels that provides the shell structure required of any central potential useful for real nuclei. If we recall that each energy level has $2(21+1)$ degenerate m states, then, by the Pauli principle, each nl level can contain $2(2l+1)$ particles. Therefore, if we imagine filling such a potential well with fermions, each group or shell can contain, at most, the specific numbers of particles indicated in the figure. Hence, such a potential automatically gives a shell structure rather than, say, a uniform distribution of levels. Unfortunately, except for the lowest few, these shells do not correspond to the empirical magic numbers. Therefore, while the harmonic oscillator potential is a reasonable first order approximation to the effective nuclear potential, it must be modified to be useful. It was in fact, the monumental achievement of Meyer and , independently, of Haxel, Jensen and Suess, to concoct a simple modification to the harmonic oscillator potential that enabled it to reproduce the empirical magic numbers. Therefore, the addition of an l^2 term is equivalent to a more attractive potential at larger radii and comes closer to the desired effect of a more constant interior potential. The relation of the single particle levels produced by a HO potential, along with the addition of an l^2 term is illustrated in the middle panel of Fig.2.1, which shows how the $2n+1$ degeneracy of the HO levels is broken as high angular momentum levels are brought down in energy.

It is clear that neither of these alternatives yet produce the magic numbers observed experimentally. so another additional term is introduced, the so called spin-orbit coupling force. With a spin-orbit component , the force felt by a given particle differs according to whether its spin and orbital angular momenta are aligned parallel or anti-parallel. If the parallel alignment is favored, and if the form of the spin-orbit potential is taken as $V_{l.s} = -V_{ls}(r)l.s$ so that it affects higher l values more,

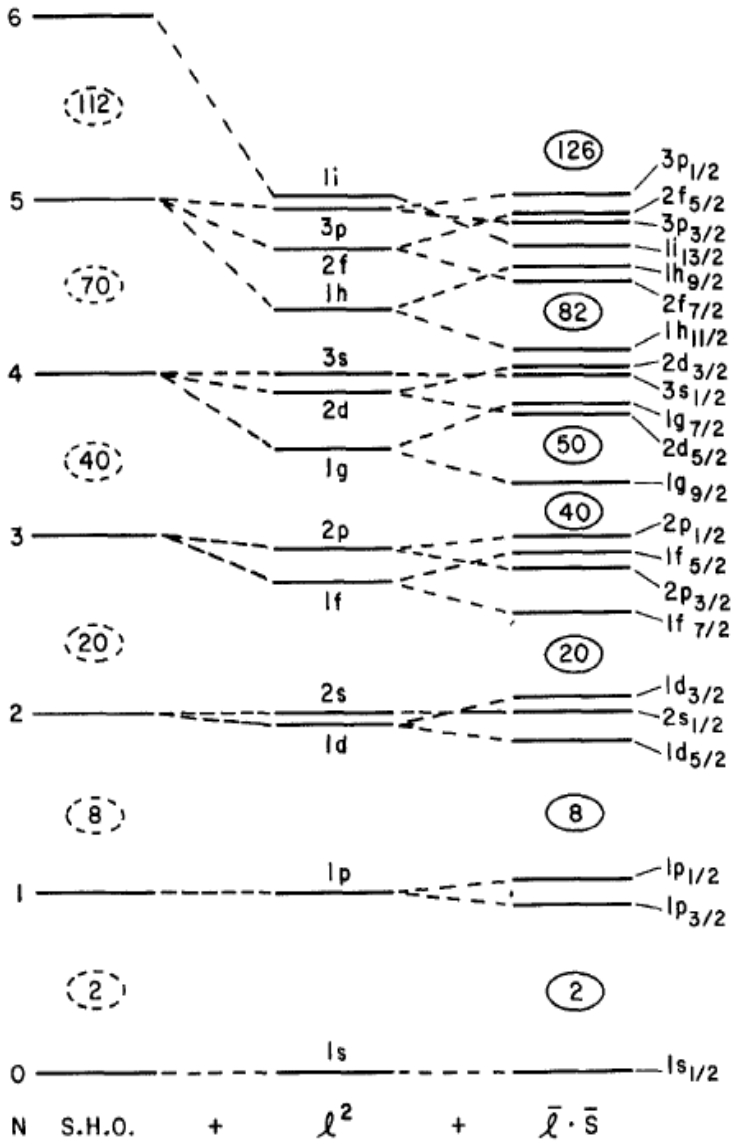

Fig.2.1 **Single-particle energies for a simple harmonic oscillator (S.H.O.), a modified harmonic oscillator with / 2 term, and a realistic shell model potential with / 2 and spin orbit (/ • *s)* terms.**

then its effects will be similar to those illustrated on the far right in Fig. 2.1. Each nl level, such as $1g$, will now be split into two, $1g_{\frac{9}{2}} and 1g_{\frac{7}{2}}$, orbits with the former lowered and the latter raised in energy. This instantly reproduces all the known magic numbers. It is therefore customary to write[1]:

$$V_{l.s} = -V_{ls}\frac{\partial V(r)}{\partial r} l.s \tag{2.1.6}$$

where $V(r)$ is whatever potential is chosen for the central potential itself and V_{ls} is a strength constant. This simple model works extremely well for a large number of nuclei. For example, by inspection of the right-hand panel of Fig. 2.2.1, we would expect the ground state of ${}^{41}_{20}Ca_{21}$, which has one neutron beyond the N = 20 closed shell, to be $\frac{7}{2}^-$. Similarly, ${}^{41}_{21}Sc_{21}$ should have a $\frac{7}{2}^-$ ground state, while the ground states of ${}^{91}_{41}Nb_{50}$ and ${}^{91}_{40}Zr_{51}$ should be $\frac{9}{2}^+$ and $\frac{5}{2}^+$, respectively. These predictions are verified experimentally.

2.1.2 Particle tri-axial rotor model

The simple model consisting of a particle coupled to a rotor provides an approximate description of many of the properties of the lowlying bands in odd-A nuclei and, at the same time, illustrates various general features of rotating systems[4]. In the particle tri-axial rotor model, the hamiltonian of an odd-A nucleus is usually written as[2,7],

$$H = H_{core} + H_{sp} + H_{pair} \tag{2.1.7}$$

In the case of triaxial deformation, the hamiltonian of the even-even core is given as,

$$H_{core} = \sum \frac{\hbar^2 R_i^2}{2J_k} = \sum \frac{\hbar^2 (I_k - j_k)^2}{2J_k} \tag{2.1.8}$$

where R, I and j are the angular momentum of the core, the nucleus and the single particle, respectively. The three rotational moments of inertia are assumed to be connected by a relation of hydro dynamical type,

$$J_k = \frac{4}{3} J_o \sin^2(\gamma + \frac{2\pi}{3}k) \tag{2.1.9}$$

where $k = 1, 2, 3$. The fixed moment of inertia J_o can be derived from the core excitation energy E_2^+. H_{sp} describes the Hamiltonian of the unpaired single particle. In the tri-axial deformed field of the even-even core, H_{sp} is given by[7],

$$H_{sp} = -\frac{\hbar^2}{2m}\nabla^2 + \frac{1}{2}m\omega_o^2 1 - 2\beta[Y_{20}\cos\gamma + \frac{1}{\sqrt{2}}(Y_{22} + Y_{2-2})\sin\gamma] - k\hbar\omega_o 2l.s + \mu(l^2 - < l_N >^2) \tag{2.1.10}$$

where k and μ are Nilsson parametres, Y_{2q} is the rank 2 spherical harmonic function. H_{pair} is the Hamiltonian to represent the pairing correlation which can be treated in the Bardeen-Cooper-Schrieffer (BCS) formalism. The single particle wave function can be expressed as

$$|\nu >= \sum C^{\nu}_{Nlj\Omega} |Nlj\Omega > \tag{2.1.11}$$

where ν is the sequence number of the single particle orbitals, $|Nlj\Omega >$ represents the corresponding Nilsson state, $C^{\nu}_{Nlj\Omega}$ is the coefficient to identify the configuration mixing. Diagonalizing the single particle Hamiltonian in the basis $|Nlj\Omega >$, we can obtain the $C^{\nu}_{Nlj\Omega}$ and the single particle eigen value ε_ν. The corresponding quasi-particle energy can then be determined by

$$E_\nu = \sqrt{(\varepsilon_\nu - \lambda)^2 + \triangle^2} \tag{2.1.12}$$

with $\lambda and \triangle$ being the Fermi energy and the energy gap, respectively. The total hamiltonian in eq(2.2.7) can be diagonalized in the symmetrically strong coupling

basis

$$|IKM\nu>=\sqrt{\frac{2I+1}{16\pi^2}}\sum C^{\nu}_{Nn_z\bigwedge\Omega}D^{I}_{MK}|Nn_z\bigwedge\omega>+(-1)^{I+K}D^{I}_{M-K}|Nn_z\bigwedge\omega> \tag{2.1.13}$$

where $\alpha^{\dagger}_{\nu}$ is creation of the single nucleon in the orbital $|\nu>$, D^{I}_{MK} is the rotational matrix.

2.1.3 Nuclear Collective model

The nuclei with $A < 150$ are generally treated interms of a model based on vibrations about a spherical equilibrium shape, while nuclei with A between 150 and 190 show structures most characteristic of rotations of a non spherical system. Vibrations and rotations are the two types of collective nuclear motion[3]. The collective nuclear model is often called "liquid drop"model, for the vibrations and rotations of a nucleus resemble those of a suspended drop of liquid and can be treated with a similar mathematical analysis. Due to my concern, let's see vibrational states roughly and rotational states relatively in detail.

Nuclear vibrations

Imagining a liquid drop vibrating at high frequency, we can get a good idea of the physics of nuclear vibrations. Although the average shape is spherical, the instantaneous shape is not. It is convenient to give the instantaneous coordinate $R(t)$ of a point on the nuclear surface at (θ, ϕ), interms of the spherical harmonics $Y_{\lambda\mu}(\theta, \phi)$. Each spherical harmonic component will have an amplitude $\alpha_{\lambda\mu}(t)$:

$$R(t) = R_{av} + \sum\sum \alpha_{\lambda\mu}(t)Y_{\lambda\mu}(\theta, \phi) \tag{2.1.14}$$

The $\alpha_{\lambda\mu}$ are not completely arbitrary; reflection symmetry requires that $\alpha_{\lambda\mu} = \alpha_{\lambda-\mu}$ and if we assume the nuclear fluid to be incompressible, further restrictions apply. The constant ($\lambda = 0$) term is incorporated into the average radius R_{av}, which is just $R_o A^{\frac{1}{3}}$. The $\lambda = 1$, $\lambda = 2$, $\lambda = 3$ vibrations are known as a dipole, quadrupole and Octapole vibrations, respectively.

Nuclear rotations

Rotational motion can be observed only in nuclei with non spherical equilibrium shapes. These nuclei can have substantial distortions from spherical shape and often called *deformed nuclei*[3,5]. They are found in the mass ranges $150 < A < 190$ and $A > 220$. The odd mass nuclei in these regions also have quadruple moments that are unexpectedly large.

Nuclear Deformation

The simplest and most commonly occurring type of deformation in nuclei is quadruple[6]. The interplay between short-range nuclear force, long-range repulsive Coulomb force, and centrifugal stretching due to rotation may well favor a non spherical or deformed equilibrium shape. In general, spherical nuclei are found around closed shells. A closed shell nucleus is formed when all the single-particle states in a group are fully occupied. When this condition is met, the total M-value, the projection of spin along the quantization axis, of the nuclear state is zero. Such an object is then invariant under a rotation of the coordinate system and must, therefore, be spherical in shape. On the other hand, for nuclei in regions between closed shells, many single-particle states are available. In this case, it may be more favorable for a nucleus to minimize its energy by going to a deformed shape. In general, the nuclear shape tends

to be prolate, i.e., elongated along the z-axis, at the beginning of a major shell and oblate, i.e., flattened at the poles, toward the end. This comes from a preference, arising from the pairing term in nuclear force, for nucleons to occupy single-particle states with the largest absolute m-values, starting from $m = j$. As a result, there is an increase in the probability at the beginning of a shell to find nucleons in the polar regions. Quantum mechanically, there cannot be a rotational degree of freedom associated with a spherical object. For a sphere, the square of its wave function is, by definition, independent of angles-it appears to be the same from all directions. As a result, there is no way to distinguish the wave functions before and after a rotation. Rotation is therefore not a quantity that can be observed in this case and, consequently, cannot correspond to a degree of freedom in the system with energy associated with it. In contrast, rotational motion of a deformed object, such as an ellipsoid, may be detected, for example, by observing the changes in the orientation of the axis of symmetry with time[6].

Rotational Bands

A nucleus in a given intrinsic state can rotate with different angular velocities in the laboratory. A group of states, each with a different total angular momentum J but sharing the same intrinsic state, forms a *rotational band*. Since the only difference between these states is in their rotational motion, members of a band are related to each other in energy, static moments, and electromagnetic transition rates. In fact, a rotational band is identified by these relations. The energy of a rotational state is given by;

$$E_J = \frac{\hbar^2}{2I} J(J+1) + E_k \tag{2.1.15}$$

where E_k represents contributions from the intrinsic part of the rotational wave function. From eq. (a) we see that the energy of a member of a rotational band is proportional to $J(J+1)$, with the constant of proportionality related to the moment of inertia I. The quantity E_k enters only in the location of the band head , the position where the band starts. Different bands are distinguished by their moments of inertia and by the positions of their band heads.

2.2 Nuclear angular momentum and parity assignment

2.2.1 Angular momentum

The total angular momentum of a nucleus containing A nucleons would be the vector sum of the angular momenta of all the nucleons[3]. This total angular momentum is usually called the **nuclear spin** and is represented by the symbol **I** and the total angular momentum of a single nucleon is represented by **j**. It will often be that a single valence particle determines all of the nuclear properties; in that case, I=j. In other cases, it may be necessary to consider two valence particles, in which case $I = j_1 + j_2$, and several different resultant values of I may be possible. Sometimes the odd particle and the remaining core of nucleons each contribute to the angular momentum, with $I = j_{particle} + j_{core}$. One important restriction on the allowed values of I comes from considering the possible z components of the total angular momentum of the individual nucleons. Each j must be half integral(1/2,3/2,5/2...) and thus its only possible z components are likewise half integral($\pm 1/2\hbar, \pm 3/2\hbar, \pm 5/2\hbar, ...$). If we have an even number of nucleons, there will be an even number of half-integral components, with the result that the z component of the total I can take only integral

values. This requires that I itself be an integer. If the number of nucleons is odd, the total z component must be half integral and so must the total I. We therefore require the following rules;

Odd A nuclei : I=half integral

even A nuclei : I=integral

2.2.2 Parity assignment

Along with the nuclear spin, the parity is also to label nuclear states. The parity(π) can take either $+(even)$ or $-(odd)$ values.

Parity=+ve(even) means the reversed state would look the same as the original

Parity=-ve(odd) means the reversed state differs from the original

Like the spin we regard the parity π as an overall property of the whole nucleus. It can be directly measured using a variety of techniques of nuclear decays and reactions. The parity is denoted by a + or - superscript to the nuclear spins, as I^{π}. There is no direct theoretical relationship between spin and parity. The parity of nuclear ground states can usually be determined from the shell model. Thus,

Even-even nuclides have even parity.

Odd-A nuclei have one unpaired nucleon . The parity is $(-1)^l$, where l is the orbital angular momentum of the unpaired nucleon.

For odd-odd nuclei , the parity is given by $(-1)^{l_1+l_2}$), where l_1 and l_2 are the orbital angular momentum of the unpaired proton and neutron.

Chapter 3

Materials and Methodology

3.1 Materials

During this study the following materials were used;

- Fortran 77 based nuclear structure code,
- Experimental data from ENSDF,
- Different data sources like journals, Physical reviews, books and etc.
- Computer
- printer
- flash and
- stationary materials

3.2 Methodology

3.2.1 Experimental data

Different reference materials have been visited for the purpose of finding experimental data. The experimental data uploaded in the cite ENSDF (Evaluated Nuclear

Structure Data files) have been used.

3.2.2 Computation

Using a computational code, Particle Tri-axial Rotor model code , numerical calculation of level energies, B(M1) and B(E2) transition probabilities and gamma branching ratios have been made. Different input data were generated and the data which gives the best fit with the experimental data was chosen. The output obtained during the best fit input data have been used for analysis.

The PTRM code has three parts;

1. Program GAMPYN
    - Calculates the single particle energies wave functions and matrix elements.
    - The input includes Nilsson parameters and nucleon numbers (k, μ),
2. Program ASYRMO
    - The input is output data from GAMPYN and number of Z, number of A, I_{min}, I_{max} and so on.
    - It diagonalise the particle plus tri axial rotor hamiltonian in strong coupling basis, with the single particle matrix elements.
3. Program PROBAMO
    - Input data
        - ▶ single particle quantities from GAMPN
        - ▶ Particle rotor quantities from ASYRMO

- Calculates both diagonal and off-diagonal matrix elements(static moments, transition rates, mixing ratios, etc)

3.2.3 Analytical Method

The resulting output of level energies, gamma transition energies and intensity branching ratio from the particle triaxial rotor model code, had been presented in table and graphs. Finally, the results were compared with the experimental data.

3.2.4 Data analysis

The resulting output from the particle tri-axial rotor model was presented in tables and figures representing the level diagrams. The energy of each level, gamma transition energy and transition probabilities was displayed in graphs. Finally, the result have been compared with the experimental data.

Bibliography

[1] RF.Casten:*Nuclear structure from a simple perispective* , Oxford university press,1990

[2] Eur.phys.J.A36,127-130(2008)

[3] Kenneth S. Krane:*Introductory Nuclear Physics* , Origon state University, 1988

[4] Bohr,A. and Motelson,B.:*Nuclear structure vol.II*, word scientific, 1999

[5] Nuclear Physics principles and application, John Liley,2001

[6] Samuel S.M.Wong:*Introductory Nuclear physics* 2^{nd} *edition*, John Wiley, 1998

[7] P.Ring, and P.Schuck: *The Nuclear many-body problem*, Springer-verlag,Newyork Inc.,1980

[8] I.Ragnarsson,and Paul Semmes: *The particle tri-axial rotor model*: A users guide, Tenessee technological University press, 1992

[9] Lawrence Berceley; *A guide to the nuclear science wall chart*, 2003

[10] James Rainwater; Phys.rev.79,432(1950)

[11] M.shamsuzzoha Basunia NDS 102,719(2004)

[12] F.G Kondev NDS 98,801(2003)

[13] S.-c.Wu NDS 106,367(2005)

Chapter 4
Result and discussion

In this work, the theoretical calculation of level energies, gamma transition energies and intensity branching ratios of low-lying states of three Osmium isotopes, (^{175,177,181}Os), were performed by using particle tri-axial rotor model (PTRM}with the help of fortran77 based codes called GAMPYN, ASYRMO and PROBAMO. The calculation is processed by varying the Nilsson parametres in order to bring a good agreement of the calculated values with that of experimental data.

The experimental data which used in this work was taken from [11], [12] and [13] for ^{175}Os ,^{177}Os and ^{181}Os respectively. The calculation have been done for low-lying states of two rotational bands from each selected Osmium isotopes. The calculation result is discussed as follows by using tables and graphs in comparison with experimental data.

4.1 Results and discussion of lowlying states for ^{175}Os

^{175}Os(Z = 76, N = 99, A = 175) has more than three rotational bands which were identified experimentally. But for this study the lowlying states were taken from two -ve parity lowlying rotational bands, that is, from Band(A):5/2[512] and Band(B):1/2[521] rotational bands of ^{175}Os. The experimental and theoretical values of level energy, gamma transition energy and intensity branching ratios of those states of the bands are as follows.

4.1.1 Experimental Values

The values of level energy and gamma transition energy of the low-lying states of the two bands of ^{175}Os were taken from ENSDF (Evaluated Nuclear Structure Data Files) which was evaluated by M.Sham Suzzoha Basunia in 2004 and were given in the Table 4.1.1 . The level scheme diagram of the experimental Values of the lowlying states of the two lowlying rotational bands of ^{175}Os were plotted in the Fig. 4.1.1 a) and b).

Table 4.1.1 Experimental values of ^{175}Os

Rotational Bands											
Band(A): 5/2[512]						Band(B):1/2[521]					
J^{π}_i	Ei	J^{π}_f	E_f	Eγ	Iγ	J^{π}_i	Ei	J^{π}_f	E_f	E_γ	Iγ
$7/2^-$	90.3	$5/2^-$	0	90.3	100	$3/2^-$	175.6	$1/2^-$	102.3	73.3	
$9/2^-$	207.5	$7/2^-$	90.3	117	42	$5/2^-$	193.76	$3/2^-$	175.6	18.16	
		$5/2^-$	0	207.5	100			$1/2^-$	102.3	96	
$11/2^-$	346.5	$9/2^-$	207.5	139	60	$7/2^-$	355.86	$5/2^-$	193.76	162.1	
		$7/2^-$	90.3	256	100			$3/2^-$	175.6	180	
$13/2^-$	504.7	$11/2^-$	346.5	158	59	$9/2^-$	381.56	$7/2^-$	355.86	25.7	
		$9/2^-$	207.5	297	100			$5/2^-$	193.76	183	
$15/2^-$	679.8	$13/2^-$	504.7	175	27						
		$11/2^-$	346.5	333	100						

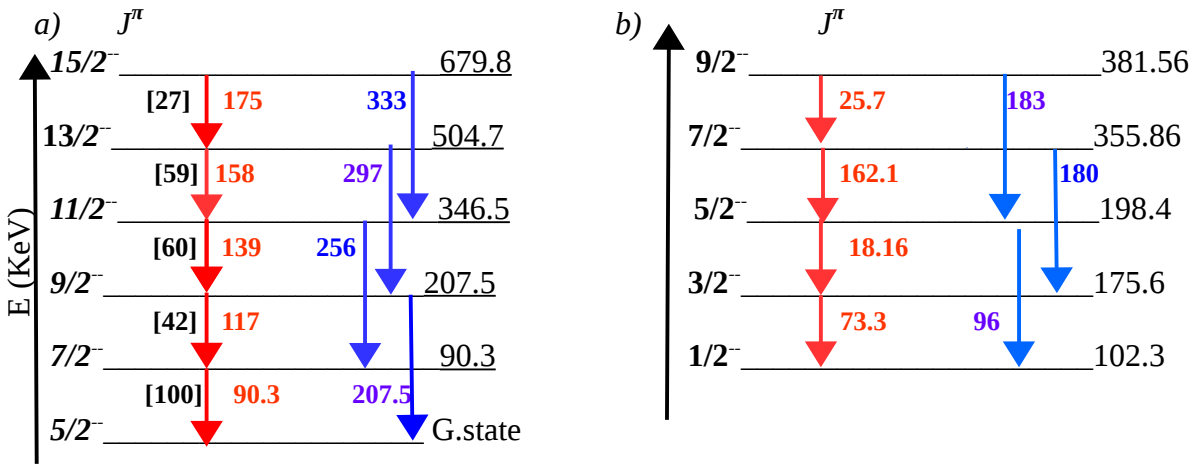

Fig. 4.1.1 Experimental level schemes of bands a) 5/2[512] and b) 1/2[521] of ^{175}Os

4.1.2 PTRM Calculation result for ^{175}Os

Using a nuclear structure computational code , Particle tri-axial rotor model(PTRM) , the level energies, gamma transition energies and intensity branching ratio of the low-lying states of the lowlying rotational bands of ^{175}Os were calculated. The output were displayed in Table 4.1.2 . The PTRM calculated level shem was given in fig. 4.1.2 .

Table 4.1.2 Calculation results of two ^{175}Os bands

Rotational Bands											
Band(A): 5/2[512]						Band(B):1/2[521]					
J^{π}_i	Ei	J^{π}_f	E_f	Eγ	Iγ	J^{π}_i	Ei	J^{π}_f	E_f	E_γ	Iγ
$7/2^-$	97.0	$5/2^-$	0	97.0	100	$3/2^-$	173.3	$1/2^-$	102.3	71	100
$9/2^-$	196.8	$7/2^-$	97.0	100	27	$5/2^-$	198.4	$3/2^-$	173.3	25.1	21
		$5/2^-$	0	196.8	100			$1/2^-$	102.3	96	100
$11/2^-$	344.3	$9/2^-$	196.8	148.3	22	$7/2^-$	352	$5/2^-$	198.4	153.6	43
		$7/2^-$	97.0	247	100			$3/2^-$	173.3	25.1	100
$13/2^-$	503.1	$11/2^-$	344.3	158.5	17.4	$9/2^-$	387	$7/2^-$	352	35	9
		$9/2^-$	196.8	306	100			$5/2^-$	198.4	188.6	100
$15/2^-$	679.7	$13/2^-$	503.1	176.6	56						
		$11/2^-$	344.3	335	100						

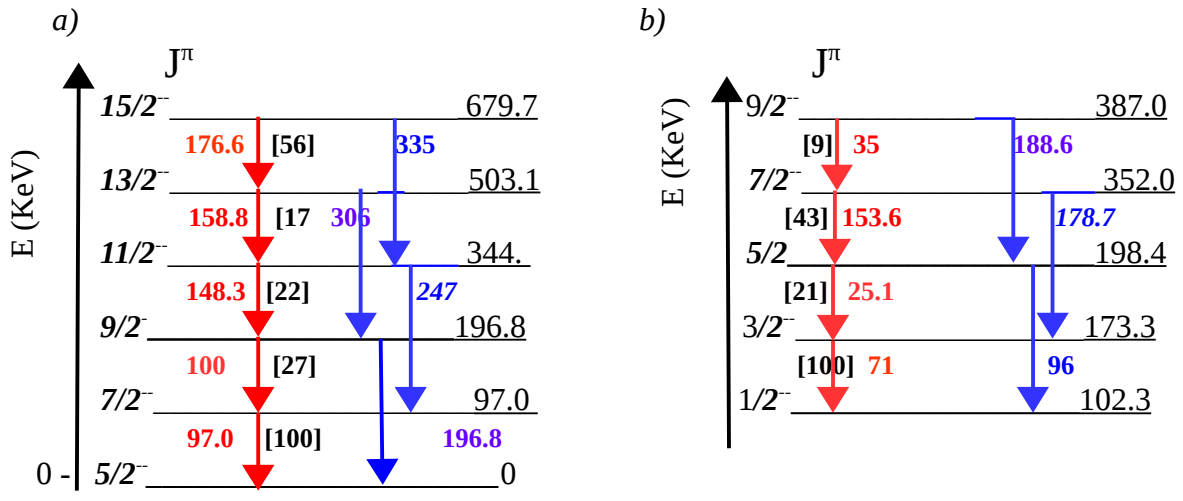

Fig. 4.1.2 Calculated level shemes of Bands a) 5/2[512] b) 1/2[521] of ^{175}Os

4.1.3 Comparison between the Experimental and PTRM calculation results of ^{175}Os

The PTRM calculated level energies for the lowlying states of ^{175}Os agree well with the experimental level energies. The comparison between the experimental and the PTRM calculation values were given in Table 4.1.3 i) and 4.1.3 ii) with its schem diagram in Fig. 4.1.1 and 4.1.2 i) and ii) for the low-lying states of the two bands ^{175}Os .

Table 4.1.3 i) Experimental and Theoretical values of rotational band, band(A):5/2^{-}[512], of ^{175}Os.

J_i	E_i		J_f	E_f		$E\gamma$		$I\gamma$	
	Exp.	Cal.		Exp.	Cal.	Exp.	Cal.	Exp.	Cal.
7/2$^-$	90.3	97.0	**5/2$^-$**	0	0	90.3	97.0	100	100
9/2$^-$	207.5	196.8	**7/2$^-$**	90.3	97.0	117	100	42	27
			5/2$^-$	0	0	207.5	196.8	100	100
11/2$^-$	346.5	344.3	**9/2$^-$**	207.5	196.8	139	148.3	60	22
			7/2$^-$	90.3	97.0	256	247	100	100
13/2$^-$	504.7	503.1	**11/2$^-$**	346.5	344.3	158	158.5	59	17.4
			9/2$^-$	207.5	196.8	297	306	100	100
15/2$^-$	679.8	679.7	**13/2$^-$**	504.7	503.1	175	176.6	27	56
			11/2$^-$	346.5	344.3	333			

Table 4.1.3 ii) Experimental and Theoretical values of rotational band, band(B):1/2[521], of ^{175}Os.

J^{π}_i	**E_i** (KeV)		J^{π}_f	**E_f**(KeV)		**$E\gamma$** (KeV)	
	Exp.	Calc.		Exp.	Calc.	Exp.	Calc.
3/2^{--}	175.6	173.3	**1/2^{--}**	102.3	102.3	73.3	71
5/2^{--}	193.76	198.4	**3/2^{--}**	175.6	173.3	18.16	25.1
7/2^{--}	355.86	352.0	**5/2^{--}**	193.76	198.4	162.1	153.6
9/2^{--}	381.56	387.0	**7/2^{--}**	355.86	352.0	25.7	35

As can be seen from Table 4.1.3 i) and Table 4.1.3 ii) the PTRM calculated level energy for the level $9/2^-$ in the band, Band(A): **$5/2^{--}$[512] ,** deviates more from experimental value compared to the energies of other levels. While in the band , Band(B):**1/2[521] ,** the PTRM calculated level energy again for level $9/2^-$ deviates more from experimental value compared to the other energy levels.

Gamma transition energies of PTRM calculated levels in both bands has values nearer to the experimentally obtained values, except; i) in band(A) for the transition from level 9/2 to 7/2, in which PTRM calculation gives 100 KeV gamma transition energy while experimentally the gamma energy was 117 KeV. ii) in band(B) for the transition from level 9/2 to 7/2, in which PTRM calculation results 35 KeV gamma transition while the experimental gamma energy was 25.7 KeV.

The gamma intensity branching ratio of all the transitions were calculated using PTRM code but, not all transitions have experimental gamma branching ratio. The branching ratios for transition $\Delta I = 2$ was taken as 100 in both PTRM calculation and experimental. But for $\Delta I = 1$ transitions the calculated data for both bands and the experimental data only for Band(A) were displayed in the tables (Table 4.1.3 i) and in square bracket [ ] in the level scheme, Fig. 4.1.2. i) . When we see the comparison between the PTRM calculation of the gamma intensity branching ratio of band(A) and the experimental value, the transition from level 13/2 to 11/2, the theoretical value has a slight deviates compared to other transitions.

4.2 Results and discussion for low-lying states of ^{177}Os

The low-lying states of Osmium-177 (^{177}Os) for this work were selected from two lowlying rota-tional bands; Band(A):1/2[521] and Band(B):5/2[512]. The experimental and the PTRM calculation values were given below.

4.2.1 Experimental data for ^{177}Os

The values of level energy and gamma transition energy of the low-lying states of the two bands of ^{175}Os were taken from ENSDF (Evaluated Nuclear Structure Data Files) which was evaluated by F.G Kondev in 2003 and were given in the Table 4.2.1 . The level scheme diagram of the experimental Values of the lowlying states of the two lowlying rotational bands of ^{175}Os were plotted in the Fig. 4.2.1 a) and b).

Table 4.2.1 Experimental values of level energies of two ^{177}Os bands

Rotational Bands											
Band(A): 1/2[521]						**Band(B):5/2[512]**					
J^{π}_i	**Ei**	**J^{π}_f**	**E_f**	**Eγ**	**Iγ**	**J^{π}_i**	**Ei**	**J^{π}_f**	**E_f**	**E_γ**	**Iγ**
3/2$^-$	75.6	**1/2$^-$**	0	75.6		**7/2$^-$**	240.4	**5/2$^-$**	152.3	88	
5/2$^-$	90.6	**3/2$^-$**	75.6	15		**9/2$^-$**	355.3	**7/2$^-$**	240.4	115	
		1/2$^-$	0	90.6				**5/2$^-$**	152.3	203	
7/2$^-$	259.2	**5/2$^-$**	90.6	168		**11/2$^-$**	494.5	**9/2$^-$**	355.3	139	
		3/2$^-$	75.6	183.6				**7/2$^-$**	240.43	254	
9/2$^-$	285.1	**7/2$^-$**	259.2	26		**13/2$^-$**	655.9	**11/2$^-$**	494.5	161	
		5/2$^-$	90.6	194.5				**9/2$^-$**	55.3	300	
11/2$^-$	534	**9/2$^-$**	285.1	249							
		7/2$^-$	259.2	274							
13/2$^-$	567.5	**11/2$^-$**	534	33.5							
		9/2$^-$	285.1	282							

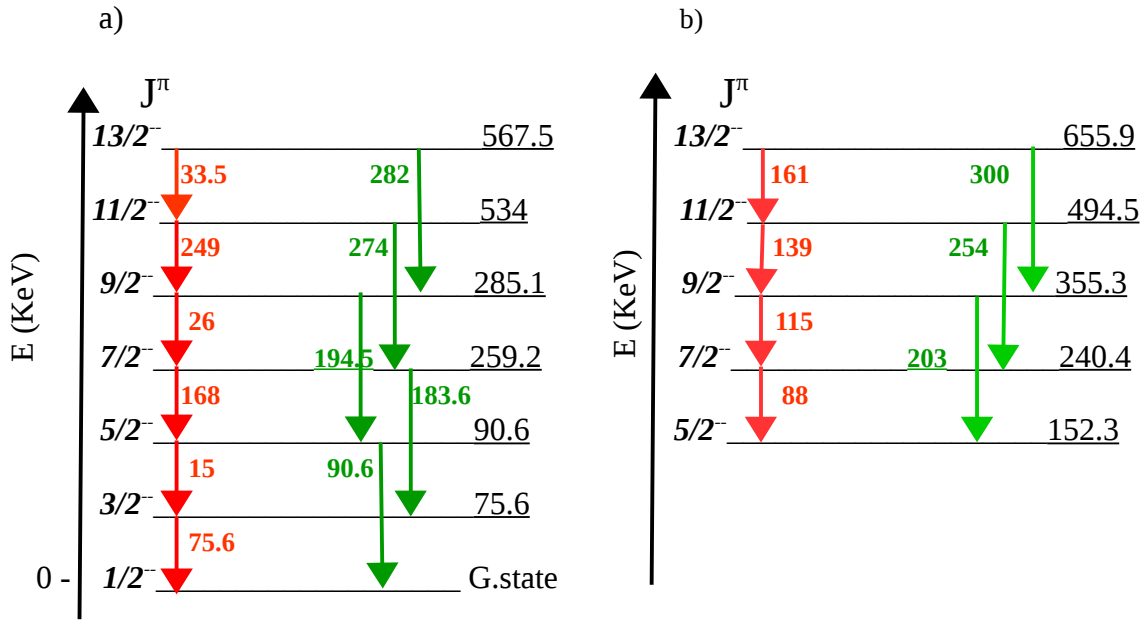

Fig. 4.2.1 Experimental values of level energies of a) Band(A):1/2[521] and b) Band(B):5/2[512] of 177-Os

4.2.2 PTRM calculation results for ^{177}Os

Using Particle tri-axial rotor model (PTRM) code, the level energies, gamma transition energies and intensity branching ratio of the low-lying states of the lowlying rotational bands of ^{177}Os were calculated. The results of those quantities were displayed in Table 4.2.2 . And also the PTRM calculated level scheme was given in Fig. 4.2.2 .

Table 4.2.2 Calculated level energy values of rotational bands of ^{177}Os

Rotational Bands											
Band(A): 1/2[521]						Band(B):5/2[512]					
J^{π}_i	Ei	J^{π}_f	E_f	Eγ	Iγ	J^{π}_i	Ei	J^{π}_f	E_f	E_γ	Iγ
3/2⁻	75.6	**1/2⁻**	0	75.6	100	**7/2⁻**	242.1	**5/2⁻**	148.8	93.3	100
5/2⁻	92.8	**3/2⁻**	75.6	17	2.3	**9/2⁻**	348.8	**7/2⁻**	242.1	107	37
		1/2⁻	0	92.8	100			**5/2⁻**	148.8	200	100
7/2⁻	259.2	**5/2⁻**	92.8	166	18	**11/2⁻**	493.7	**9/2⁻**	348.8	145	53
		3/2⁻	75.6	183.6	100			**7/2⁻**	242.1	251.6	100
9/2⁻	280	**7/2⁻**	259.2	21	3.2	**13/2⁻**	651.3	**11/2⁻**	493.7	158	8
		5/2⁻	92.8	187.2	100			**9/2⁻**	348.8	302	100
11/2⁻	530	**9/2⁻**	280	250	7						
		7/2⁻	259.2	271	100						
13/2⁻	557.9	**11/2⁻**	530	28	5						
		9/2⁻	280	278	100						

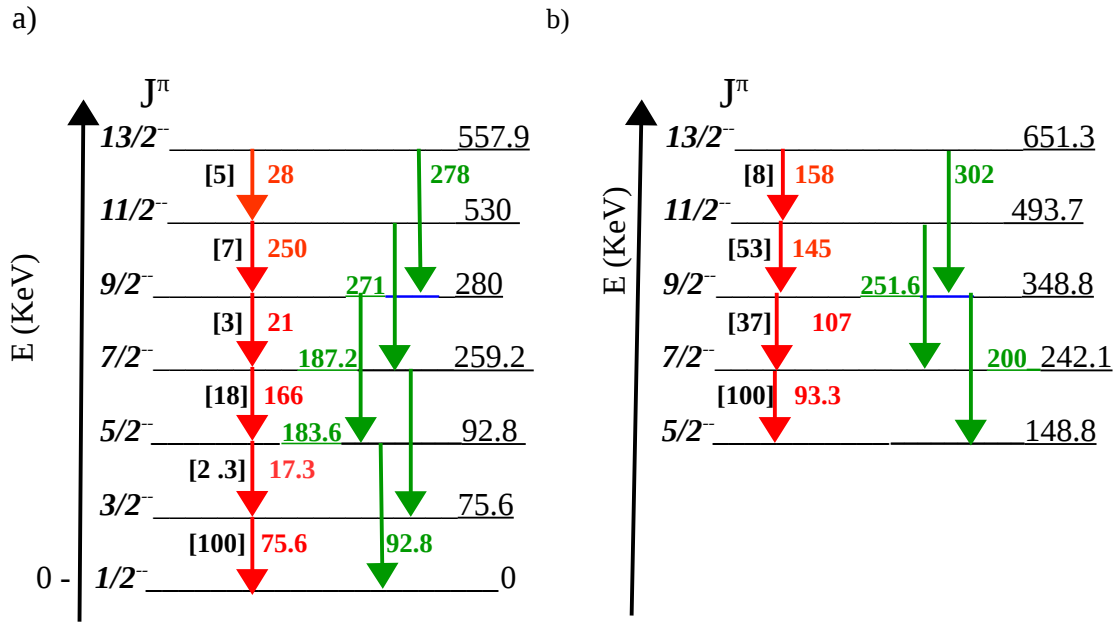

Fig. 4.2.2 Theoretical values of level energies of a) Band(A):1/2[521] and b) Band(B):5/2[512] of 177-Os

4.2.3 Comparison between the measured and PTRM calculation results of ^{177}Os

The PTRM calculated level energies for the lowlying states of ^{177}Os agree well with the experimental level energies. The comparison between the experimental and the PTRM calculation values were given in Table 4.2.3 i) and 4.2.3 ii) for the low-lying states of the two bands of ^{177}Os .

Table 4.2.3 i) Comparison between Experimental and Theoretical level energy of rotational band, band(A):1/2[521], of ^{177}Os.

J^{π}_i	E_i (KeV)		J^{π}_f	E_f(KeV)		$E\gamma$ (KeV)	
	Exp.	Calc.		Exp.	Calc.	Exp.	Calc.
3/2^{--}	75.6	75.6	**1/2 $^{--}$**	0	0	75.6	75.6
5/2^{--}	90.6	92.8	**3/2^{--}**	75.6	75.6	15	17
7/2^{--}	259.2	259.2	**5/2^{--}**	90.6	92.8	168	166
9/2^{--}	285.1	280	**7/2^{--}**	259.2	259.2	26	21
11/2^{--}	534	530	**9/2^{--}**	285.1	280	249	250
13/2	567.5	557.9	**11/2^{--}**	534	530	33.5	27.9

As it was given in the Table 4.2.3 i) and Table 4.2.3 ii) the PTRM calculated level energy for the level 13/2^{-} in the band, Band(A): **5/2^{--}[512] ,** has a larger deviation from experimental value comparatively. For Band(B):**1/2[521] ,** the PTRM calculated level energy for level 9/2^{-} deviates more from experimental value compared to the other energy levels.

Table 4.2.3 ii) Comparison between Experimental and calculated values of band, band(B):5/2[512], of ^{177}Os.

J^{π}_i	E_i (KeV)		J^{π}_f	E_f(KeV)		$E\gamma$ (KeV)	
	Exp.	Calc.		Exp.	Calc.	Exp.	Calc.
7/2^{--}	240.4	242.1	**5/2 $^{--}$**	152.3	148.8	88	93.3
9/2^{--}	355.3	348.8	**7/2^{--}**	240.4	242.1	115	107
11/2^{--}	494.5	493.7	**9/2^{--}**	355.3	348.8	139	145
13/2^{--}	655.9	651.3	**11/2^{--}**	494.5	493.7	161	158

Gamma transition energies($E\gamma$) of PTRM calculated levels in both rotational bands has values nearer to the experimentally obtained values, except; i) in band(A) for the transition from level 13/2 to 11/2, in which PTRM calculation gives 27.9 KeV gamma transition energy while experimentally the gamma energy was 33.5 KeV. ii) in band(B) for the transition from level 9/2 to 7/2, in which PTRM calculation results 107 KeV gamma transition while the experimental gamma energy was 115 KeV.

The gamma intensity branching ratio of all the level transitions for ^{177}Os were calculated using PTRM code for transition of $\Delta I = 1$. But for $\Delta I = 2$ it was taken as 100 in PTRM calculation and the results were displayed in the Table 4.2.2 .

since we were unable to find the experimental data for the gamma intensity branching ratios, it was unable to draw a comparison for ^{177}Os.

4.3 Result and discusion for low-lying states of ^{181}Os

As for the above two Osmium isotopes, the low-lying states for this work were taken from two lowlying rotational bands; Band(I):1/2[521] and Band(E):7/2[514] of 181 Os. The experimental and the calculated values of level energy, gamma transition energy and branching ratio of those states were given below.

4.3.1 Experimental Values

The experimental Values of level energies, gamma transition energies and intensity branching ratios of lowlying states of ^{181}Os were taken, from ENSDF (Evaluated Nuclear Structure Data Files). The data was evaluated in Aug. 2005 by S.-C.Wu and was given in Table 4.3.1 . The level scheme diagram of the experimental Values of the lowlying states of the two lowlying rotational bands of **^{181}Os** were plotted in Fig. 4.3.1 a) and b).

Table 4.3.1 Experimental values of level energies of two ^{181}Os bands

Rotational Bands											
Band(I): 1/2[521]						**Band(E):7/2[514]**					
J^{π}_i	Ei	J^{π}_f	E_f	Eγ	Iγ	J^{π}_i	Ei	J^{π}_f	E_f	E_γ	Iγ
3/2$^-$	93.9	**1/2$^-$**	0	93.9		**9/2$^-$**	172.76	**7/2$^-$**	49.2	123.5	100
7/2$^-$	320.93	**5/2$^-$**	102.76	218.17		**11/2$^-$**	321	**9/2$^-$**	172.76	148.3	28
		3/2$^-$	93.9	227				**7/2$^-$**	49.2	271.8	100
9/2$^-$	334.26	**7/2$^-$**	320.93	13.3		**13/2$^-$**	491.34	**11/2$^-$**	321	170.4	7.8
		5/2$^-$	102.76	231				**9/2$^-$**	172.76	318.5	100
11/2$^-$	663.65	-	-	-		**15/2$^-$**	682.33	**13/2$^-$**	491.34	191	6.2
		7/2$^-$	320.93	342.7				**11/2$^-$**	321	361	100
13/2$^-$	677.22	-	-	-		**17/2$^-$**	891	**15/2$^-$**	682.33	209	4.8
		9/2$^-$	334.26	343				**13/2$^-$**	491.34	400	100

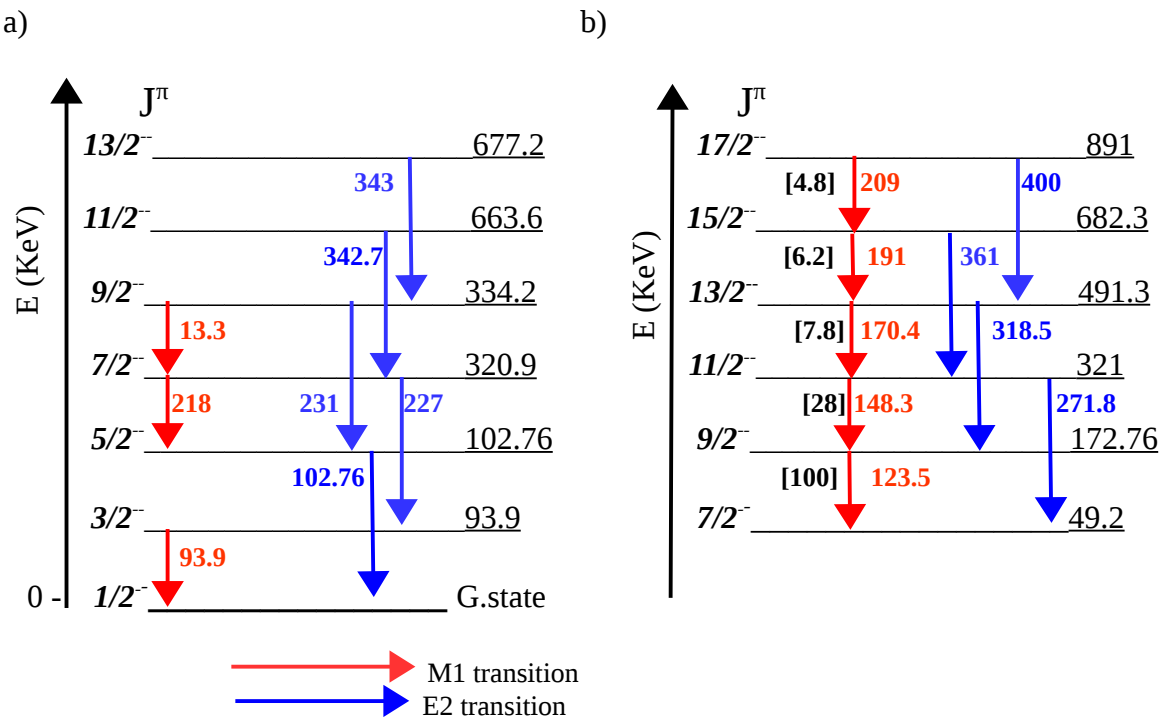

Fig. 4.3.1 Experimental values of level energy of rotational band a) Band(I):1/2[521] and b) Band(E):7/2[514] of 181-Os

4.3.2 PTRM calculation results for ^{181}Os

By using PTRM calculation, the level energy, gamma transition energy and intensity branching ratio of lowlying states of lowlying rotational bands for ^{181}Os were calculated.

The output of the codes was given in Table 4.3.2. The level schemes was also drawn in Fig.4.3.2.

Table 4.3.2 Theoretical Values of level energies of two ^{181}Os bands

Rotational Bands											
Band(I): 1/2[521]						Band(E):7/2[514]					
J^{π}_i	Ei	J^{π}_f	E_f	Eγ	Iγ	J^{π}_i	Ei	J^{π}_f	E_f	E_γ	Iγ
$3/2^-$	93.6	$1/2^-$	0	93.6	100	$9/2^-$	173.3	$7/2^-$	48.6	124.7	100
$7/2^-$	320.2	$5/2^-$	106.5	213.7	21	$11/2^-$	323.8	$9/2^-$	173.3	150.5	9.4
		$3/2^-$	93.6	226.6	100			$7/2^-$	48.6	275	100
$9/2^-$	339.0	$7/2^-$	320.2	18.8	78	$13/2^-$	501.7	$11/2^-$	323.8	177.9	3
		$5/2^-$	106.5	232.5	100			$9/2^-$	173.3	328	100
$11/2^-$	654.2	-	-	-	-	$15/2^-$	687.3	$13/2^-$	501.7	185.6	3.7
		$7/2^-$	320.2	334.0	100			$11/2^-$	323.8	363.5	100
$13/2^-$	671.6	-	-	-	-	$17/2^-$	880.5	$15/2^-$	687.3	193	1.9
		$9/2^-$	339.0	333.0	100			$13/2^-$	501.7	379	100

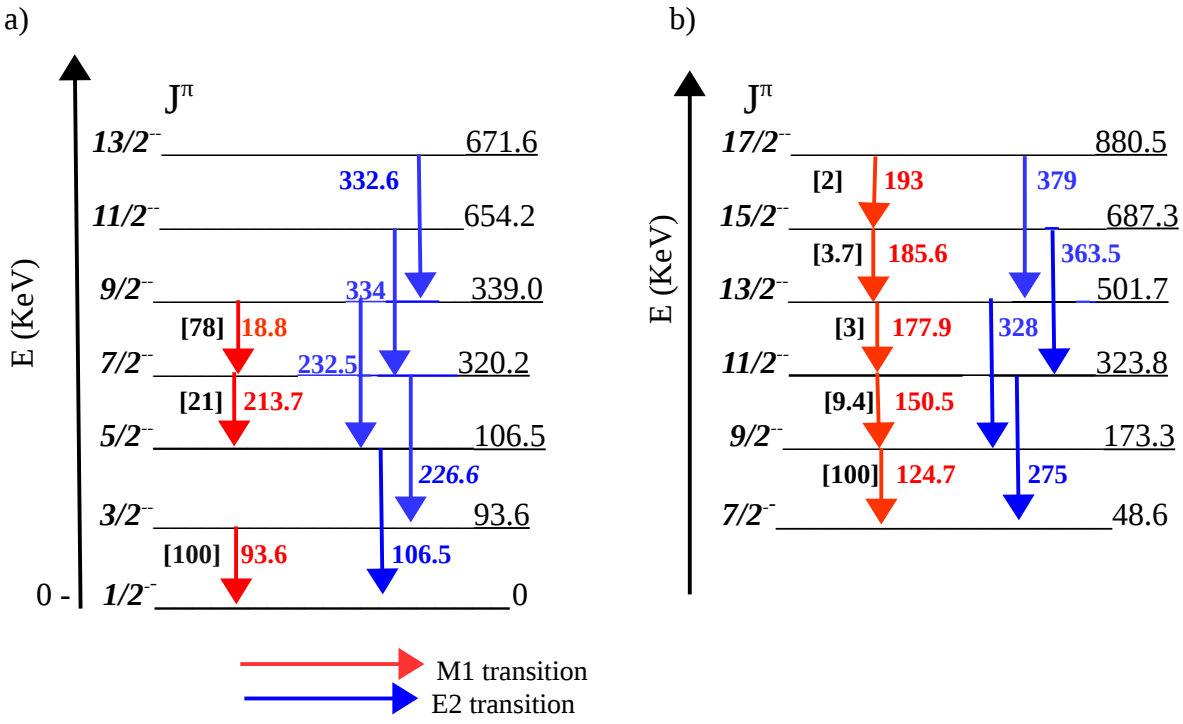

Fig. 4.3.2 Calculated level scheme of rotational bands a) (Band(I):1/2[521]) and b) Band(E):7/2[514] of 181-Os

4.3.3 Comparison between the PTRM result and the experimental data for ^{181}Os

As it was given in Table 4.3.3 i) and Table 4.3.3 ii) the PTRM calculated level energy for the level $11/2^-$ in the band, Band(I): $1/2^-$**[521] ,** deviates more from experimental value compared to the energies of other levels. While in the band , Band(E):**7/2[514] ,** the PTRM calculated level energy again for level $17/2^-$ deviates more from experimental value compared to the other energy levels.

Table 4.3.3 i) Comparison between Experimental and Theoretical level energy of rotational band, band(I):1/2[521], of ^{181}Os.

J^{π}_i	E_i (KeV)		J^{π}_f	E_f(KeV)		$E\gamma$ (KeV)	
	Exp.	Calc.		Exp.	Calc.	Exp.	Calc.
3/2	93.9	93.6	**1/2**	0	0	93.9	93.6
$7/2^-$	320.93	320.2	**$5/2^-$**	102.76	106.5	218.17	213.7
$9/2^-$	334.26	339.0	**$7/2^-$**	320.93	320.2	13.3	18.8
$11/2^-$	663.65	654.2	**$7/2^-$**	320.93	320.2	342.7	334.0
$13/2^-$	677.22	671.6	**$9/2^-$**	334.26	339.0	343	333.0

Gamma transition energies of PTRM calculated levels in both bands has values in a good agreement with that of the experimentally obtained values, except; i) in band(I) for the transition from level $13/2^-$ to $9/2^-$, in which PTRM calculation gives 333 KeV gamma transition energy while experimentally the gamma energy was 343 KeV. ii) in band(E) for the transition from level $17/2^-$ to $15/2^-$, in which PTRM calculation results 193 KeV gamma transition while the experimental gamma energy was 209 KeV.

The gamma intensity branching ratio of all the transitions were calculated using PTRM code but, not all transitions have experimental gamma branching ratio. The branching ratios for transition $\Delta I = 2$ was taken as 100 in both PTRM calculation and experimental. But for $\Delta I = 1$ transitions the calculated data for both bands were given in Table 4.3.2 ii) and displayed in square bracket in the level scheme of Fig. 4.3.2.

Table 4.3.3 ii) Comparison between Experimental and Theoretical value of rotational band, band(E):7/2[514], of ^{181}Os.

J_i	E_i		J_f	E_f		$E\gamma$		$I\gamma$	
	Exp.	Cal.		Exp.	Cal.	Exp.	Cal.	Exp.	Cal.
9/2$^-$	172.7	173.3	**7/2$^-$**	49.2	48.6	123.5	124.7	100	100
11/2$^-$	321	323.8	**9/2$^-$**	192.7	173.3	148.3	150.5	28	9.4
			7/2$^-$	49.2	48.6	271.8	275	100	100
13/2$^-$	491.34	501.7	**11/2$^-$**	321	323.8	170.4	177.9	7.8	3
			9/2$^-$	192.7	173.3	318.5	328	100	100
15/2$^-$	682.33	687.3	**13/2$^-$**	491.34	501.7	191	185.6	6.2	3.7
			11/2$^-$	321	323.8	361	363.5	100	100
17/2$^-$	891	880.5	**15/2$^-$**	682.33	687.3	209	193	4.8	1.9
			13/2$^-$	491.33	501.7	400	379	100	100

From the two rotational bands of ^{181}Os in concern, we have found the experimental value of the gamma intensity branching ratio only for band(E). When we compare the branching ratio of the gamma transition from level 11/2 to 9/2 the PTRM calculated gamma intensity branching ratio of the band is smaller compared to the experimental value.

CHAPTER 5

CONCLUSION

In this thesis the lowlying states for three odd mass Osmium isotopes have been calculated using PTRM . Different trials have been made on the calculation by shifting the input data slightly from the previous. The best input data which gives approximatly regenerates the experimental data have been saved in the computer and the output of the data were given in tables and discussed using graphs. From the result of the calculation the following conclusion were drawn.

- PTRM calculation for the lowlying states of ^{175}Os agrees in level energy and gamma transition energy . But slight shift have been observed between PTRM calculation and experimental data of intensity branching ratio of band(B). For band(B), since we are unable to find experimental data of intensity branching ratio, comparison were not drawn.
- From the PTRM calculation for lowlying states of ^{177}Os, a well agreement between the PTRM calculation and experimental data were observed for level energies and gamma transition energies. However the PTRM calculation for intensity branching ratio of the lowlying states were performed, since we are unable to find its experimental value the comparison was not drawn.
- PTRM calculation for the lowlying states of ^{181}Os agrees in gamma transition energy and level energy. But there were a slight shift between the PTRM calculation and theexperimental value.

Table of Contents

List of Tables

List of Figures